

# INTERNATIONAL SOCIETY FOR SOIL MECHANICS AND GEOTECHNICAL ENGINEERING



*This paper was downloaded from the Online Library of the International Society for Soil Mechanics and Geotechnical Engineering (ISSMGE). The library is available here:*

<https://www.issmge.org/publications/online-library>

*This is an open-access database that archives thousands of papers published under the Auspices of the ISSMGE and maintained by the Innovation and Development Committee of ISSMGE.*

*The paper was published in the proceedings of the 20<sup>th</sup> International Conference on Soil Mechanics and Geotechnical Engineering and was edited by Mizanur Rahman and Mark Jaksa. The conference was held from May 1<sup>st</sup> to May 5<sup>th</sup> 2022 in Sydney, Australia.*

# On the behaviour of rock berms to arrest axial walking of offshore pipelines

## Sur le comportement des bermes de roche pour arrêter la marche axiale de pipelines offshore

Colm O'Beirne, Phil Watson & Conleth O'Loughlin

University of Western Australia, WA, Crawley, Western Australia, Australia

Meysam Banimahd & Matthew Kuo

Woodside Energy, WA, Perth, Western Australia, Australia

**ABSTRACT:** Subsea pipelines are used to transport gas (and fluids) from subsea wells to processing facilities. Over the life of a project, cycles of operation and shutdown can lead to axial 'walking' of pipelines and potential damage to facilities. Rock berms may be used to mitigate walking, by adding weight to increase the frictional restraint of the pipeline against the seabed. Recent studies (by others) have identified the potential for 'arching' to occur within the berm, linked to pipeline embedment, which reduces the stress applied to the pipeline and may thereby reduce the magnitude of axial restraint for a fixed volume of rock. To overcome reductions in axial restraint, longer rock berms may be required thereby increasing project costs.

The objective of the current study is to investigate the extent to which arching may impact the effectiveness of rock berms to mitigate walking. The method used was physical modelling in a geotechnical centrifuge. The results presented in this paper specifically investigate whether pipeline embedment can lead to arching in 'real' rock berms, and whether associated axial movement may lead to 'collapse' of the arch and reinstatement of the restraint. Results were obtained using a specially designed trapdoor model and are presented from testing of different berm geometries at centrifuge accelerations of 20g and 10g. The study concludes that arching can occur in response to pipeline embedment, but that this can 'recover' in response to axial movement of the pipeline. The degree of recovery depends on the amount of embedment adopted.

**KEYWORDS:** Rock berm, axial resistance, arching, pipeline walking, centrifuge modelling, trapdoor

## 1 INTRODUCTION

Rock berms installed on and around subsea pipelines are widely used for various applications including protection against external impacts, stability under environmental loads, global buckling and restraint against axial 'walking'. The latter phenomenon is caused by cyclic expansion and contraction driven mainly by heating and cooling, and where frictional resistance at the seabed creates a bias for axial movement of a pipeline in one direction over the other (see Carr et al. 2006 and Bruton et al. 2010). Over the life of a project, cycles of operation and shutdown can cause significant cumulative axial displacement leading to potential failures at connections to pipeline end termination facilities and manifolds.

Mitigation of axial walking depends on the active pressure applied by the rock berm. This is opposed to the passive resistance for most other applications, where the berm anchoring effectiveness is mobilised as the pipeline itself moves orthogonally. Plainly, should contact be lost at the pipe-rock interface, the friction (or 'grip') to restrain axial walking could be lost.

Recognising the tendency for a pipeline to embed deeper into the seabed with axial cycles (White et al. 2011), recent numerical studies by Carneiro et al. (2017) and Rodriguez et al. (2018) have reported potential 'arching' effects. Here, the pipeline embeds independently leading to stress redistribution within the berm, resulting in arching over the pipe crown where the rock is self-supported. A simple schematic of the arching phenomenon is given in Figure 1, showing a reduction in pipe/berm contact area and a loss of berm effectiveness to arrest pipeline walking.

Physical modelling literature on the arching phenomenon is lacking. The first objective of the current study was to identify if arching can occur for 'real world' berm geometries. The second was to quantify any resultant reduction of axial restraint provided by the rock berm to the pipeline. The final objective was to investigate if axial movement of the pipeline reduces the effects of arching, causing the berm to 'collapse' back onto the pipeline crown. Meeting these objectives will allow for improvements to design methodology.

Centrifuge modelling at the National Geotechnical Centrifuge Facility, UWA was used to efficiently examine berm setup variables for a specific offshore project. Obtaining similitude between the model and field stress (and strain) conditions allows realistic performance data to be gathered. This is achieved in centrifuge testing by reducing the dimensions of the model by a factor,  $N$ , whilst increasing the acceleration level by the same factor,  $N$ . Hence, for this study the stresses within the berm and the stresses applied to the seabed from the weight of the berm are scaled correctly.

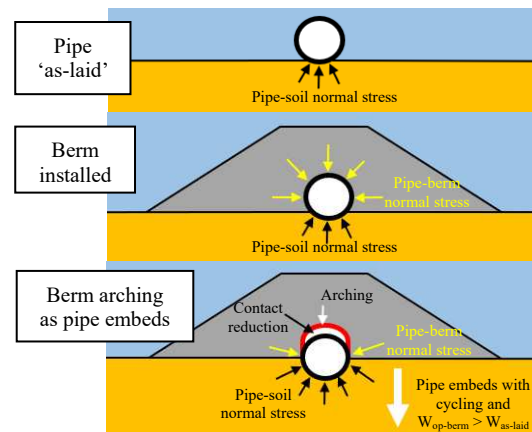


Figure 1. Simple schematic of arching mechanism

## 2 PHASED TESTING APPROACH

### 2.1 Complex system of forces

Figure 1 shows where friction would be generated along both the pipe-seabed and pipe-berm interfaces. The system of normal contact stresses acting on subsea pipelines is complex and depends on the internal stresses of the berm. The following

requires consideration when determining the amount of axial restraint available:

1. Pipe-berm interaction: Arching within the berm as the pipeline embeds relative to the base of the berm may reduce the axial restraint, although cycling could cause the rock to ‘collapse’ back onto the pipeline.
2. Pipe-seabed interaction: Cyclic hardening at the pipeline-soil interface can increase the interface resistance (for a given normal load).
3. Berm-seabed interaction: Compression of the soil beneath the berm, which would be greatest towards the location of the pipeline, could result in secondary arching in the rock above the pipe.

### 2.2 Isolate restraint components

Considering the complexity of quantifying the available axial restraint, the test programme was divided across three phases to isolate restraint components. Phase 1 comprised ‘trapdoor’ experiments to consider arching within various ‘real’ rock berms independently of the seabed response, while Phases 2 and 3 comprised tests on a representative soft offshore clay soil. This paper presents the Phase 1 trapdoor tests using a locally acquired gravel to model the berm. A comprehensive interpretation of Phase 2 and 3 is in progress, together with other trapdoor tests using materials of different angularity/sphericity.

The trapdoor tests were carried out in the 3.6 m diameter beam centrifuge, at accelerations of 20g and 10g, i.e. prototype dimensions are scaled down by 20 or 10 respectively. A complete description of this centrifuge, as commissioned in 1989, is provided by Randolph et al. (1991). Variations of pipe vertical and axial displacement magnitudes, rates and sequencing were investigated together with variations in berm geometry.

## 3 MODEL AND SETUP

### 3.1 Trapdoor apparatus

The removal of support from the base of a soil profile has been successfully examined by means of physical models using trapdoor experiments since Terzaghi (1936). The current study involves manipulation of a model pipe using a 2-directional actuator allowing both vertical (changes in pipe embedment) and horizontal (axial pipeline walking) movements to be imposed on the pipe. As shown in Figure 2, static ‘table-tops’ are situated either side of the pipe to simulate a rigid ‘seabed’, with the gap between the table-top edges acting as the ‘trapdoor’ for the pipe to be moved through. A specific rock berm geometry is formed on the table-tops and over the pipe crown before each test inside a strongbox featuring a front Perspex viewing window. High-resolution photography provides a means of visualising pipe/berm movements, while vertical and axial loads acting on the pipe from the rock berm are continuously measured.

The pipe is rigidly connected to a pipe stand, having a width equal to the outer diameter of the pipe, which prevents model berm particles escaping (or becoming wedged) in the trapdoor opening, i.e. between the pipe and the edges of the table-tops. This is particularly important for pipe ‘embedments’ of  $\leq 0.5D$ . The pipe stand is connected to load cells mounted to a loading frame (see Figure 2). The frame translates vertical and horizontal movements from the actuator, moving the pipe independently of the stationary table-tops. As the model pipe is shorter than the 225 mm deep strongbox to allow for axial displacements, short lubricated aluminium hoods are placed over the pipe crown as shown in Figure 2 to prevent gravel particles escaping (or becoming trapped) between the pipe ends and the strongbox front/back walls. The hoods slide through notches formed in the table-top edges, with tolerances to allow vertical movement of the hoods with the pipe, while restricting their movement in the

axial direction. The testing arrangement allows for vertical displacements of  $0D$  to  $0.7D$  and up to 6 mm ( $\pm 3$  mm from centre) axial displacement.

### 3.2 Pipe and instrumentation

Two model pipes of hollowed aluminium tube were tested, with outer diameters of 17 mm and 34 mm, lengths of approximately 12 & 6 diameters and wall thicknesses of 2.75 mm and 5.5 mm for testing at 20g and 10g respectively (i.e. prototype outer diameter of 0.34 m). The pipes were anodised to prevent damage during the submerged testing, resulting in an average surface roughness of  $0.51 \mu\text{m}$ .

The vertical and axial loads transferred to the pipeline were detected by two sets of load cell pairs, with each pair located close to the end of the model pipe. Each load cell pair comprised an S-type load cell with a measurement range of 1 kN to measure vertical load and a beam type load cell with a measurement range of 200 N to measure axial resistance.

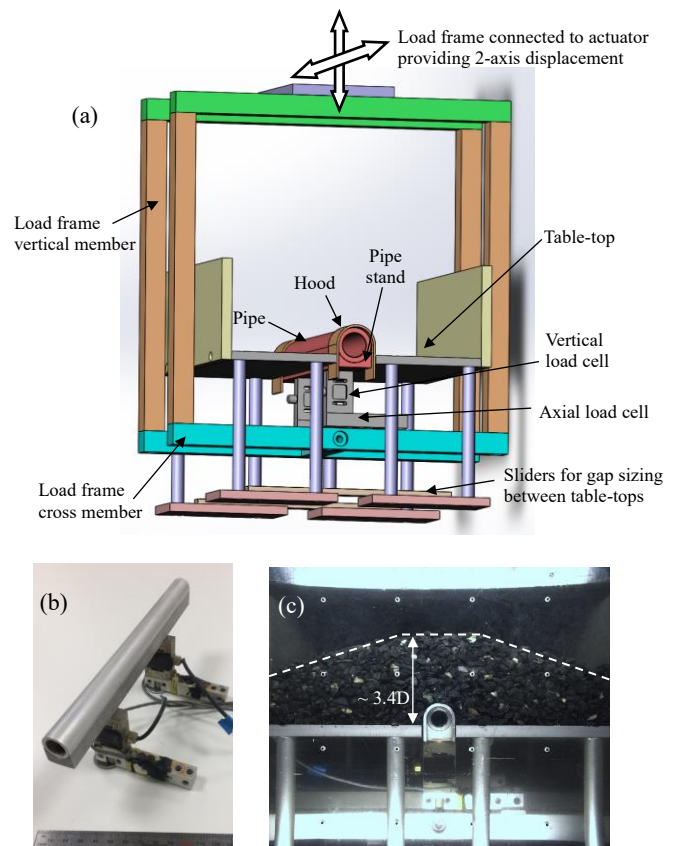


Figure 2. Apparatus: (a) drawings for fabrication (b) pipe and instrumentation (c) berm at testing acceleration

### 3.3 Berm geometry and material

Two berm configurations were tested, both having crest widths of  $2.9D$  but different heights ( $2.2D$  and  $3.4D$ ) and slopes ( $1:3$  and  $1:4$ ). The larger berm (in-flight) is shown on Figure 2c.

The gravel was of granitoid origin from the Hanson Byford quarry, Western Australia and exhibits a unit weight similar to natural rock. Its properties are summarised in Table 1 with a sub-sample photo given in **Error! Reference source not found.** Separate blends were used in the 20g tests ( $1:20$  blend) and 10g tests ( $1:10$  blend). Laboratory testing carried out in accordance with relevant Australian Standards (AS 1289.3.6.1) generated the grading curves presented in Figure 3. Two-dimensional (2D) particle aspect ratios were measured using definitions provided in CIRIA (2007).

Table 1. Gravel properties

Parameter	Value
Specific gravity	2.7 (-)
Bulk dry unit weight	15.4 (kN/m <sup>3</sup> )
Angle of repose	37 – 39 (°)
Angularity   Sphericity (tactile assessment)	sub-angular to angular   0.4 – 0.6 (-)
2D aspect ratio	1.45 (-)
Colour	Dark blue to grey, trace white

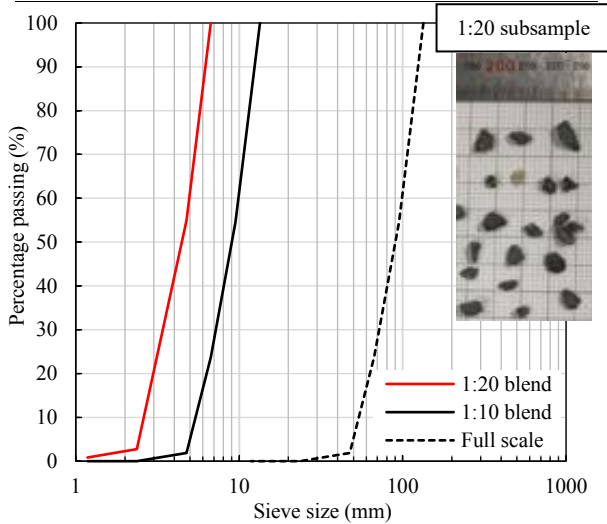


Figure 3. Rock grading curves

### 3.4 Testing procedures

Each trapdoor test comprised the following:

- i. with the centrifuge stopped, position the table-tops either side of the pipe stand while ensuring small (~0.3 mm) gaps between the table edges and pipe stand to reduce any unwanted apparatus friction;
- ii. position the lubricated pipe hoods over the pipe crown and through the table-top notches, adjust the load frame (located on the actuator) to target a specified initial pipe ‘embedment depth’, and install the berm by pouring wet gravel (from the specified gravel blend) from a constant height above the table-tops to target a constant berm density; using a 3D printed profiler to achieve the correct berm geometry;
- iii. submerge the apparatus in water to above the berm crest and zeroing load cells at 1g, then spin the centrifuge to the required acceleration level and allow approximately 10 minutes for the system and load cell data to equilibrate before starting the test.

## 4 SELECT RESULTS AND DISCUSSION

During the initial ramp-up to target acceleration, a (very) slight ‘flex’ in the load frame was observed, resulting in (near imperceptible) downward displacement of the pipe relative to the rigid ‘seabed’. This led to a lower vertical load than would be anticipated based on the berm geometry, and provided the first clue that arching is a real mechanism. To compensate for the flex, the pipe was raised slightly (to a target vertical load) before continuing with the test.

### 4.1 Onset of arching

Lowering the pipe at a constant rate (all testing is drained) yielded a rapid drop in vertical load, approaching 0 kN/m, and is

indicative of arching within the rock berm. Corresponding video footage captured during the tests confirms cavity propagation over the pipe crown.

Sensitivity checks on the effect of initial pipeline embedment relative to the berm base were completed. Figure 4a shows good agreement across tests when applying a constant lowering embedment rate and implies that initial embedment depth does not influence the potential for (or behavior of) arching. For each initial embedment depth, additional tests were performed that included axial cycling of the pipeline, and at face value, axial cycles do not appear to influence the arching mechanism.

The axial resistances in Figure 4b were measured in tests where a drop in vertical load to ~0 kN/m was observed. The axial resistance would therefore be expected to be negligible, and the observations are reasonably consistent with friction between the pipe and the hoods (which was confirmed by calibration testing). In each test, axial displacements of  $\pm 0.18D$  were applied via 5 axial cycles over the embedment range for each test (i.e. the cyclic frequency was varied to limit the cyclic to 5 cycles).

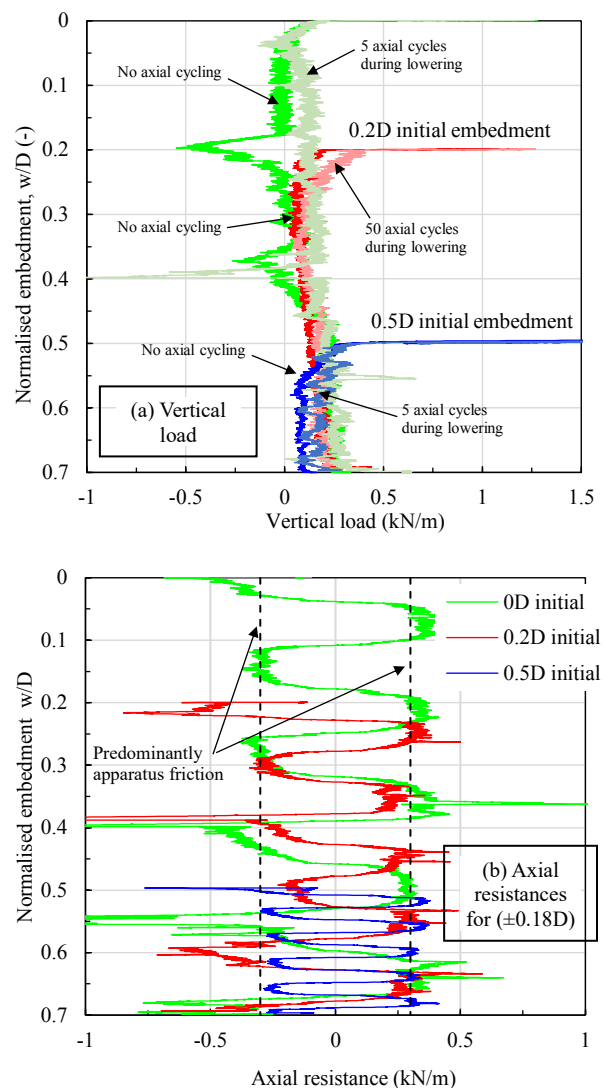


Figure 4. Various initial embedment depths in same berm size

### 4.2 Influence of berm size

Negligible influence on the arching mechanism was observed for berms of different size. Figure 5a appears to show a slightly lower vertical load with embedment for the larger berm where no axial cycling of the pipeline was applied. While this could imply

that larger berms can lead to greater arching, the difference is negligible (possibly within the range expected from slight changes in apparatus setup), and when the same tests were done with axially cycling, little difference was observed (see Figure 5 b). Based on this, it seems that berm size does not contribute to arching, at least for the range examined in this project.

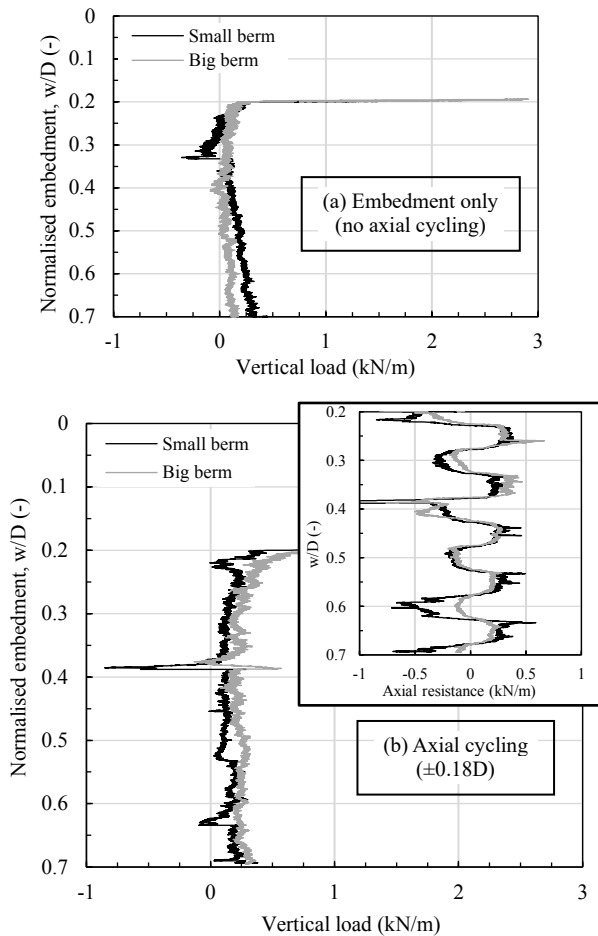


Figure 5. Influence of berm size

#### 4.3 Indication of arching ‘collapse’

The axial cycle sequence incorporated at the beginning of ‘Test B’ in Figure 6 provides the initial evidence that cycling could lead to restraint ‘recovery’.

Both ‘Test A’ and ‘Test B’ in Figure 6 begin with the same minor upwards raise of the pipeline to around 1.2 kN/m. For ‘Test B’, this was directly followed by axial cycling of the pipeline at a constant  $w/D$  (i.e. no embedment). During this stage, the vertical load increased to approximately 1.7 kN/m; an increase of greater than 40%. The ultimate value is within 5% of the vertical load that might be estimated by considering the ‘block’ of rock above the pipe, which is 1.6 kN/m. In contrast, ‘Test A’ involved lowering immediately after reaching the 1.2 kN/m target, with the vertical load dropping close to zero.

On completion of the axial cycles in ‘Test B’, the pipeline was lowered similarly to ‘Test A’, and the vertical load profiles with embedment are shown to agree. This indicates that the initial sequence of axial cycles has no discernible effect on vertical load behavior over the remainder of the test (i.e. arching still occurs once axial cycling stops, and the pipeline embeds).

#### 4.4 Axial restraint recovery

Building on the ‘Test B’ findings, more involved testing was performed that comprised stages of embedment and axial cycling.

In each case, the pipes were lowered (with cycling) to a target embedment, better reflecting real-world conditions, where pipeline embedment is expected to be finite.

Figure 7 presents the vertical load and axial resistance developed in two tests, each at a different acceleration level. An overview of the test parameters/stages is given in Table 2. Both ‘Test C’ and ‘Test D’ started with an initial ‘embedment’ of 0.2D and included an initial pipeline raise to target a specific vertical load. The pipeline was then lowered (Stage 1) by 0.03D and 0.21D for Test C and Test D respectively, with continuous axial cycling. Axial cycling then continued at constant ‘embedments’ (Stage 2) until a total of 50 cycles were performed. The tests featured a third stage, where the pipeline was simply lowered further but with no axial cycling (not reflecting real-world conditions).

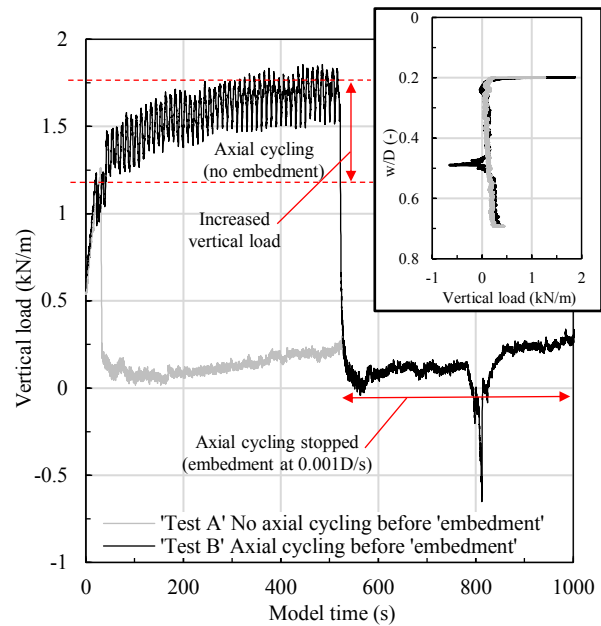


Figure 6. Vertical load increase for axial cycling at constant  $w/D$

In both tests (and for both acceleration levels) a rapid drop in vertical load was observed to (roughly) 0.5 kN/m once pipeline lowering was initiated. These vertical loads reduce further as the pipe is lowered, approaching 0 kN/m. After a vertical displacement of 0.03D, all tests are in reasonable agreement with a vertical load of around 0.25 kN/m observed. The vertical load and axial resistances reduce further for Test D, as the pipeline ‘embeds’ deeper to 0.21D.

Upon commencement of Stage 2 for Test C, a sharp increase in the vertical load is developed over the first cycle. With continued axial cycles at the fixed embedment depth in Stage 2, almost 70% of the maximum vertical load seen in Figure 6 is recovered. This load recovery is in good agreement for both acceleration levels.

A similar sharp increase in vertical load is developed over the first Stage 2 cycle of Test D. However, with continued axial cycles at fixed  $w/D$ , only 35% of the maximum vertical load is recovered. This was even less for the 10g counterpart, where the vertical load dropped all the way to 0 kN/m during embedment.

Overall, the data suggest that axial cycling can mitigate the reduction in pipe crown weight observed due to arching, and hence recover the axial restraint, although this depends on the magnitude of pipeline embedment applied. Over the first few axial cycles, the axial resistances in both tests are in agreement – as would be expected considering the displacement sequencing is consistent. However, once pipe embedment in Test C stops, the axial resistance begins to increase; whereas the axial resistance

for Test D continues to decrease after the initial few axial cycles as vertical embedment continues. On completion of Stage 1 for Test D, the axial resistance reduces to approximately 0.25 kN/m, which is thought to be close to the value of apparatus friction. Consistent with the changing vertical load, axial cycling helps to quickly recover the axial restraint offered by the rock berm, provided there is limited vertical embedment.

Table 2. Test parameter overview (use with Figure 7)

Test ID	Stage	Embedment depth (D)		Model test time (s)	Axial cycles	
		Initial	Final		Frequency (Hz)	No. cycles
C	1	0.2	0.23	30	0.1	3
	2	0.23	0.23	470		47
	3	0.23	0.70	470	0.0	0
D	1	0.2	0.41	210	0.1	21
	2	0.41	0.41	290		29
	3	0.41	0.70	290	0.0	0

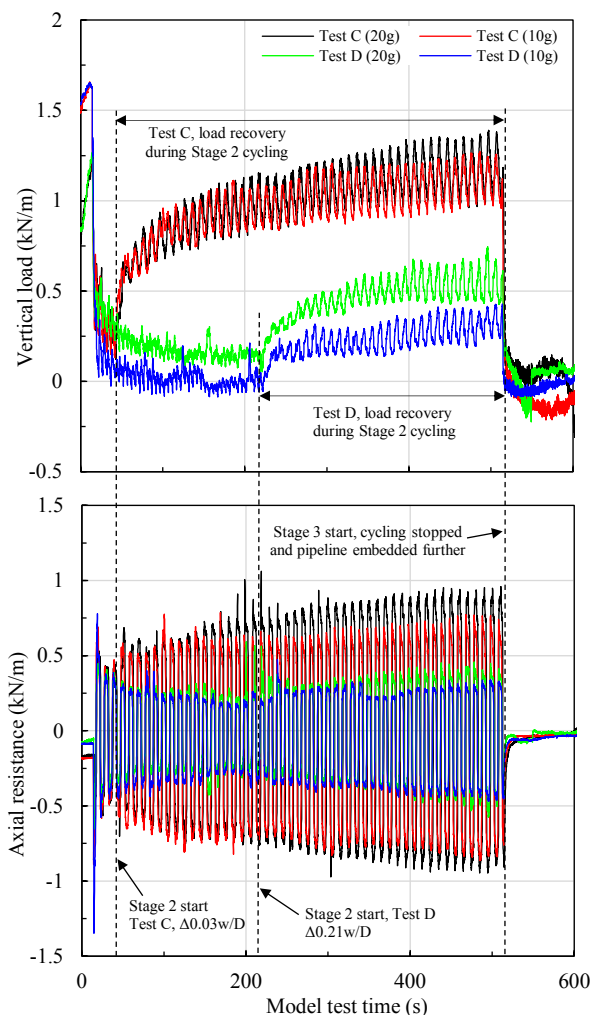


Figure 7. Axial restraint recovery

## 5 CONCLUSIONS

A centrifuge test programme was undertaken to investigate the extent to which arching may impact the effectiveness of rock berms to mitigate pipeline walking. This paper presents the outcomes from ‘trapdoor’ tests using model rock berms over a 0.34 m diameter pipe.

An arching mechanism within the rock berm was shown to occur as the pipeline ‘embeds’. Vertical loads acting on the pipeline reduced to nearly 0 kN/m as it was lowered relative to a rigid seabed. The mechanism was observed in all tests featuring a constant pipeline embedment rate.

The onset/behaviour of arching was found to be independent of initial pipeline embedment depth and berm size, and was confirmed at centrifuge accelerations of 10g and 20g. A collapse mechanism was identified whereby cycles of axial displacement led to ‘recovery’ of vertical load on the pipeline. However, the magnitude of the recovery depends on the level of pipeline embedment – and is particularly evident when the pipe is cycled axially without ongoing embedment.

A more comprehensive interpretation of this testing is in progress, together with further trapdoor results using berm material of different angularity and sphericity. The interpretation of Phase 2 and 3, each comprising tests on a representative soft offshore clay soil, is also underway.

## ACKNOWLEDGEMENTS

This research was carried out in partnership with Woodside Energy Limited. The authors thank the NGCF team for their support to this test campaign. The second author acknowledges support provided from Shell Australia via the Shell Chair in Offshore Engineering at UWA.

## REFERENCES

- Bruton, D., Sinclair, F. and Carr, M. (2010). Lessons Learned From Observing Walking of Pipelines with Lateral Buckles, Including New Driving Mechanisms and Updated Analysis Models. Offshore Technology Conference, Houston Texas, USA, 3–6 May 2010, Paper No. OTC 20750.
- Carneiro, D., Borges Rodriguez, A., Klinkvort, R. T., Worren, A. and Banimahd, M. (2017). Active Pressure of Rock Berms on Pipelines. Proc. of the 8th Int. Conf. on Offshore Site Investigation and Geotechnics (OSIG) 2017, 12-14 Sept. 2017 London.
- Carr, M., Sinclair, F., and Bruton, D. (2006). Pipeline Walking- Understanding Field Layout Challenges, and Analytical Solutions Developed for the Safebuck JIP, Offshore Technology Conference, Houston Texas, USA, 1-4 May 2006, Paper No. OTC 17945.
- CIRIA, CUR, CETMEF (2007). The Rock Manual. The use of rock in hydraulic engineering (2nd edition). C683, CIRIA, London.
- Rodriguez, A. B., Klinkvort, R. T., & Worren, A. (2018). Axial Rock Berm-Pipeline-Seabed Interactions. Offshore Technology Conference, 20-23 March, Kuala Lumpur.
- Terzaghi, K. 1936. Stress distribution in dry and saturated sand above a yielding trap-door. Proc 1st International Conference of Soil Mechanics, Harvard University, Cambridge (USA), 1: 307-311.
- White, D., Bruton, D. A. S., Bolton, M., Hill, A. J., Ballard, J.-C., and Langford, T. (2011). SAFEBUCK JIP - Observations of Axial Pipe-soil Interaction from Testing on Soft Natural Clays. Offshore Technology Conference.